

ENHANCED OSTEOBLAST FUNCTIONS ON RGD IMMOBILIZED SURFACE

Hui Huang, DDS, PhD
Yimin Zhao, DDS, PhD
Zhiguo Liu, MD, PhD
Yumei Zhang, DDS, PhD
Hui Zhang, DDS, MSc
Tao Fu, MSc
Xuanxiang Ma, DDS, PhD

KEY WORDS

RGD
Cell function
Osteoblast

Hui Huang, DDS, PhD, Yimin Zhao, DDS, PhD, Yumei Zhang, DDS, PhD, Hui Zhang, DDS, MSc, and Xuanxiang Ma, DDS, PhD, are at the Stomatological College, Fourth Military Medical University, Xi'an, China. Address correspondence to Prof. Ma at Department of Prosthodontics, Stomatological College, Fourth Military Medical University, 1, Kang Fu Road, Xi'an City 710032, China (e-mail: maxx@fmmu.edu.cn).

Zhiguo Liu, MD, PhD, is at the Xijing Hospital, Fourth Military Medical University, Xi'an, China.

Tao Fu, MSc, is at the Institute of Material Science and Engineering, Xi'an Jiaotong University, Xi'an, China.

Many methods are currently under investigation to improve the integration of dental implants to surrounding bones. Among these methods, peptide-modified surfaces have been highlighted as one of the most promising. Our study, aimed at the cellular response to RGD-immobilized surface in vitro, investigated the basis for designing a bone-active surface coating with RGD-containing peptide. Gold-coated titanium surfaces were used as indicative control surfaces for peptide immobilization. Using self-assembly monolayer techniques, 2 types of peptides, RGDC (Arg-Gly-Asp-Cys) and RDGC (Arg-Asp-Gly-Cys), were immobilized onto the gold surfaces. Surface justification was realized through X-ray photoelectron spectroscopy and Fourier transform infrared spectra. Primary calvarial osteoblasts were cultured on RGDC, RDGC, and non-peptide-coated surfaces. Cell attachment, morphology, proliferation, and expression of osteocalcin (OC) messenger RNA (mRNA) were assessed using cell counting, immunolabeling fluorescence microscopy, and Northern blot assay. Four and 8 hours after culture, cell attachment was enhanced on RGDC surfaces. Correspondingly, increased cell spreading and significantly greater cell proliferation were also observed in cells grown on the RGDC-coated surfaces. More importantly, osteoblasts on RGDC surfaces showed earlier and significant OC mRNA expression at day 15 compared with controls having the similar expression at day 21. These results provided evidence of the enhanced functions of osteoblasts cultured on the RGDC-modified surfaces, which might be effective in improving osseointegration for dental implants.

INTRODUCTION

Successful clinical use of dental implants requires the functional integration of implants with surrounding tissues. Regarding biological consequences caused by the implantation, the type and magnitude of tissue-implant interactions are determined by cellular and molecular

events at the tissue-implant interface. The biocompatibility of biomaterials is predominantly reflected by cell functions in contact with them. Although indicated as being biocompatible, many implant materials in practical use do not interact with the host tissue actively. So-called biocompatibility is still a concept of "bioinert" properties

that implies limited adverse disturbance on the surrounding tissue formation. To accelerate and enhance tissue integration and to maintain desired long-term stability, a type of specific, active, and guided tissue-implant interaction capable of inducing rapid and strong anchorage has been strongly expected.¹

Surface characteristics of materials, such as topography, chemical composition, and surface energy, play essential roles in the osteoblast's reactions to biomaterials. Treatment outcomes in dental implantology critically depend on implant surface designs that can optimize the biologic response during the whole integration mechanism.^{2,3} Many ongoing investigations are focused on the modification of the material surface. Among these, a distinctive trend is to associate bioactive agents with implant materials to change their osteo-conductibility into osteo-inductibility, and to offer more bioactive features to these biocompatible materials.

RGD was first identified as the attachment site for fibronectin and then as a ubiquitous adhesive motif in proteins throughout the body, including many bone extracellular matrix proteins such as thrombospondin, osteopontin, type II collagen, osteonectin, and bone sialoprotein. It is recognized by integrins, a heterodimeric cell membrane receptor family that uses multiple intracellular signaling pathways.⁴ It was reported that mimicking of RGD peptides adsorbed on substrate could enhance subsequent cell adhesion.⁵ It has also been shown that RGD-related peptides influence osteoblast mineralization, cytoskeleton reorganization, and migration in vitro.^{6,7} These investigations provide evidence that an implant coated with tailor-made RGD peptides is an attractive strategy for designing a new generation of proactive dental implants. This type of implant is expected to be capable of eliciting selective responses from target cell species, performing tissue regeneration, and leaving implant-tissue interaction under control. This strategy

might serve as a useful key technology for enhanced osseointegration.

In the present study, to investigate the general cellular response to RGD-coated surfaces, the strategy of self-assembly monolayers was used to covalently immobilize RGD-containing peptide RGDC and the control peptide RDGC onto gold-coated titanium surfaces. Titanium as a bulk material for bone implants is much better for the formation of osseointegration, but it is much easier to immobilize some peptides on the gold surface in a simple and cost-efficient way.⁸ Gold coating was only as a type of indicative experimental model surface for these in vitro experiments. To exclude the possible interference factors from the varieties of the substrate type, every titanium specimen was coated with gold, and only effects of the peptides on those surfaces were studied. Both X-ray photoelectron spectroscopy (XPS) and Fourier transform infrared spectra (FTIR) were used to confirm the immobilization. Primary calvarial osteoblasts were cultured on RGDC, RDGC, and non-peptide-coated surfaces. Cell counts were taken to analyze the cell attachment and proliferation. Fluorescein isothiocyanate conjugated (FITC) antibodies detecting the vaculin assembly were used to visualize cell spreading. Total RNA of the cultured cells was isolated, and Northern blot assay was used to analyze the osteocalcin (OC) messenger RNA (mRNA) expression.

MATERIALS AND METHODS

Substrate preparation

Substrates used in the present study were precleaned, 18- and 30-mm, round, commercial, pure titanium disks (NMRI, Xi'an, China). The 18-mm disks were prepared for use in cell attachment, spreading, and proliferation experiments, and the 30-mm disks were used in detecting OC mRNA expression. Twelve-nanometer-thick gold layers were prepared by electronic beam evaporation over 2 nm of titanium film. Peptides RGDC and RDGC

(Auka, Beijing, China) were dissolved in distilled, deionized water and ethanol (1:1) and adjusted to a 2 mM concentration. Disks were immersed in the solution overnight at room temperature in closed containers with gentle mixing. Gold-coated implants immersed in non-peptide-containing solution were used as controls (nonpeptide).

Surface identification

XPS (ESCALAB 220i XL, Fisons, Germany) was used to analyze the elemental composition and the bonding properties of the RGD-containing peptide coating. Power of nonmonochromatized MgK α ($h\nu = 1256.6$ eV) was 100 kw. Change compensation was attained by using an electron flood gun setting at 6 eV. The vacuum in the analysis chamber was 2.5×10^{-7} Pa. C_{1s}, N_{1s}, O_{1s}, and S_{2p} signals were acquired at constant pass energy of 20 eV. Fitting was finished with built-in software, and the binding energy of the main lines was determined with each spectrum being referenced to carbon pollution at 284.7 eV.

We performed FTIR on an EP1760 spectrometer (Hitachi, Tokyo, Japan) to detect the change of organic chemical groups on the substrate before and after immobilization. Gain, velocity, aperture, and resolution were set at 1, 1.9, 28, and 4 cm⁻¹, respectively. Apodization was set as the Happ-Genzel mode. Data were collected over a spectral range of 4000 to 1000 cm⁻¹. In both the XPS and FTIR experiments, only the nonpeptide surface was used as the control to RGDC surface.

Cell culture

The phenotype of neonatal rat calvarial osteoblasts, isolated via sequential enzymatic digestion, was confirmed by presence of alkaline phosphatase, formation of calcium phosphate mineral deposits, and production of OC. Then, osteoblasts were cultured in Dulbecco modified Eagle medium (DMEM, Gibco, Carlsbad, Calif) containing 10% fetal bovine serum (Gibco) in a humidified

fied atmosphere containing 5% carbon dioxide at 37°C. Osteoblasts at 2 to 3 passages were used in the experiments.

Cell attachment

Cells used for attachment assay were plated at a density of 1×10^4 cells/cm². After 4, 8, 12, 16, and 20 hours of growth in culture, the disks were washed with phosphate-buffered saline (PBS) to remove nonadherent cells and then transferred to new wells. The attached cells were trypsinized with 0.25% trypsin and 0.5 mM EDTA and counted in a Coulter counter (Beckman Coulter, Fullerton, Calif). Complete removal of the attached cells from the disks with trypsin-EDTA was confirmed by immunofluorescence microscopy. Results were expressed as means with SDs ($n = 5$). Significance was compared by analysis of variance (ANOVA).

Indirect immunofluorescence microscopy

Indirect immunofluorescence microscopy for vinculin assembly was performed at the initial stage of cell adhesion to detect the discrepancy in cell spreading. Incubation in PBS containing 1% (wt/vol) bovine serum albumin and 10% (vol/vol) normal goat serum (Sigma Chemical Company, St Louis, Mo) was performed to reduce nonspecific background staining. After cell seeding for 4 hours on the different substrates, the medium was removed and cells were fixed in methanol at -20°C for 6 minutes after a washing step in PBS. Two-hour incubations with monoclonal anti-vinculin hVIN-1 (Sigma) as primary and FITC anti-rat IgG (Sigma) as secondary antibodies were performed at 37°C with 3 washes in PBS between each incubation. Stained specimens were photographed with a Zeiss photomicroscope (Carl Zeiss, Oberkochen, Germany) after mounting coverslips.

Cell proliferation

Osteoblasts in DMEM supplemented with 10% fetal bovine serum were

seeded onto different substrates at a density of 0.5×10^4 cells/cm². The cells were then cultured under standard conditions for 1, 4, 7, 10, and 15 days. At the end of each of the described periods, osteoblasts were detached with trypsin-EDTA as mentioned previously. Cell numbers were counted in a Coulter counter, and the results were expressed as means with SDs ($n = 5$). Significance was compared by ANOVA.

Northern blot analysis

The total RNA of the 10-, 15-, and 21-day cultures was extracted using guanidine thiocyanate and phenol/chloroform.⁹ In particular, cells on different surfaces were scraped before using guanidine thiocyanate to prevent extracted RNA from binding to the peptide-coated disks. After the spectrophotometric measurement of the RNA, 10 µg of each total RNA was fractionated on 1% (wt/vol) agarose gels, stained with ethidium bromide, and transferred to immobilon-N membranes (Millipore, Bedford, Mass) using the capillary elution method. The membranes were hybridized with complementary DNA probes that were labeled with peroxidase using ECL systems (Amersham Pharmacia, Piscataway, NJ). All the hybridization and washing steps were performed according to the instructions for the ECL systems. Hybridized membranes were exposed to Kodak X-OMAT film. The OC complementary DNA was generously provided by Dr J. C. Wang (Department of Biochemistry, Fourth Military Medical University). The signal intensity of the autoradiograph was normalized to the GAPDH housekeeping gene.

RESULTS

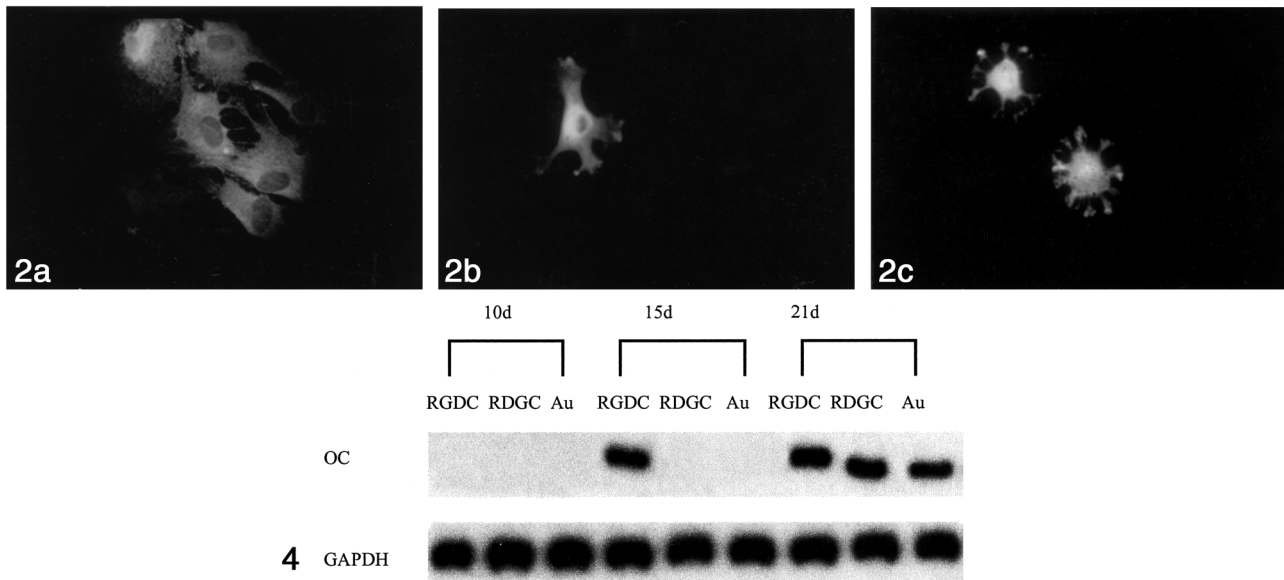
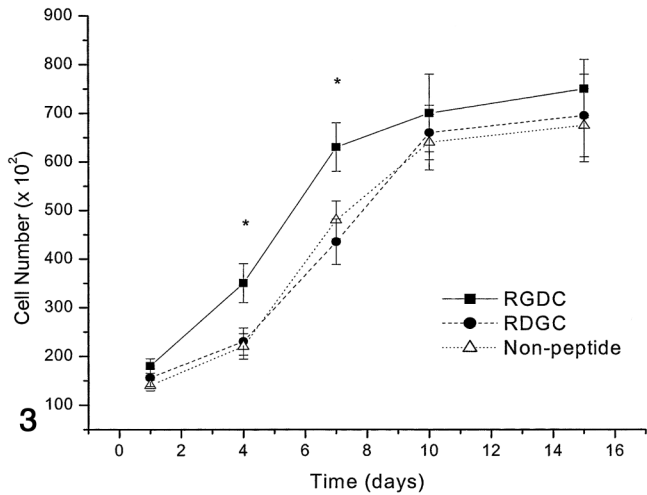
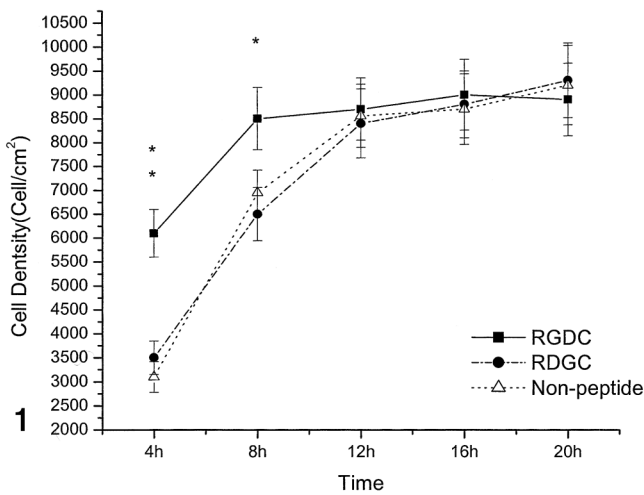
The XPS wide spectra allowed characterization of the chemical environment of the different elements. Peaks found in peptide-coated surfaces at 285.9, 288.5, 287.6, and 286.5 eV corresponded to the C_{1s} signal. Among these peaks, the major component was locat-

ed around 285.9 eV, with what might have been some other forms of carbon (C) pollution with oxygen. Nitrogen (N) clearly appeared on the RGD-containing surfaces, exhibiting a major contribution at 399.2 eV, which was typical of C-NH₂ bonding. The N/C ratio was approximately 0.25. This was much lower than the theoretical calculation of 2 from the RGDC molecule and might be explained by the high level of carbon contamination. Sulfur (S) bonding with gold was verified with S_{2p} signal spectra. A total of 80% sulfur was present as a bound thiolate with the rest in the oxidized form. The N/S ratio was approximately 7.57, which was similar to the theoretical value of 7. The O_{1s} signal appeared at 533.2 eV. Based on these major data acquired from XPS spectra, it can be confirmed that the RGDC peptide had been firmly immobilized on the substrate surface.

In FTIR spectra, characterized broad amide I stretch peak found in the 1675- to 1640-cm⁻¹ range differentiated the RGDC immobilized surfaces from controls. Moreover, on the RGDC surface, there were also some sharp and symmetric absorbance peaks found at 1735, 1281, and 964 cm⁻¹. These peaks can be attributed to the ester group (C = O) and CH₂-CH₂-COOH as well as the COOH group in Asp. All these findings confirmed the successful grafting of RGD-containing peptide onto the substrates from another aspect.

Cell attachment kinetic spotted at 4, 8, 12, 16, and 20-hour time points is shown in Figure 1 as changes of cell density (cell numbers/surface area in square centimeters). At 4 and 8 hours, obviously enhanced cell attachment was observed on RGDC-coated surfaces ($P < .01$, $P < .05$), whereas no significant difference could be found between RGDC and uncoated surfaces at mean time ($P > .05$). After 12 hours, cell attachment appeared similar on all surfaces and kept stable to the end ($P > .05$).

Assembly of vinculin during the



FIGURES 1–4. FIGURE 1. Osteoblast attachment on 3 different surfaces. Rat calvarial osteoblasts in Dulbecco modified Eagle medium (DMEM) supplemented with 10% fetal bovine serum were seeded on RGDC, RDGC, and nonpeptide surfaces at a density of 1×10^4 cells/cm² in a humidified atmosphere containing 5% carbon dioxide at 37°C. Cells were counted at 4, 8, 12, 16, and 20 hours. Values were mean \pm SEM; n = 5; Significance was compared with analysis of variance (ANOVA). ***P* < .01, **P* < .05.

FIGURE 2. Spreading pattern of osteoblasts on 3 different surfaces after 4-hour culture. Cells were labeled with monoclonal vinculin antibody hVIN-1 as primary and fluorescein isothiocyanate conjugated-labeled anti-rat IgG as secondary antibody. (a) On the RGDC surface, most osteoblasts displayed fattened pattern with nuclei clearly bounded by cytoplasm. In peripheral filopodia-like extensions, scattered vinculin-containing focal adhesions led to intimate contact between the surface and the cell. The cell spreading pattern was mature. (b) Cells on the RDGC surfaces. (c) Cells on nonpeptide surfaces. Most cells on both the RDGC and nonpeptide surfaces displayed a small and solid shape with obscure nuclei outline. Multiple rodlike projections evenly protruded outward, with vinculin spots in a punctuate circular pattern. The cell spreading pattern was immature.

FIGURE 3. Osteoblast proliferation on 3 different surfaces. Rat calvarial osteoblasts in DMEM supplemented with 10% fetal bovine serum were seeded on RGDC, RDGC, and nonpeptide surfaces at a density of 0.5×10^4 cells/cm² in a humidified atmosphere containing 5% carbon dioxide at 37°C. Cells were counted at 1, 4, 7, 10, and 15 days. Values were mean \pm SEM; n = 5; Significance was compared with ANOVA. **P* < .05.

FIGURE 4. Northern hybridization analysis of osteocalcin (OC) gene expression of osteoblasts cultured on RGDC, RDGC, and nonpeptide surfaces. The OC messenger RNA (mRNA) levels of rat calvarial osteoblasts cultured on RGDC, RDGC, and nonpeptide (gold) surfaces for 10, 15, and 21 days were determined by Northern blot assay (n = 6) as described in the "Materials and Methods" section. Equal sample loading was confirmed by normalization to the density of the GAPDH band. Cells on RGDC surfaces displayed significant early OC mRNA expression at 15 days.

initial stage of cell-surface interaction indicates great discrepancy of the osteoblast spreading pattern on different surfaces. With methanol fixation, osteoblasts exhibited a diffuse cytoplasmic immunofluorescence background staining. After 4-hour culture, cells on the RGDC surfaces demonstrated distinguished flattened pattern with the nuclei clearly bounded by cytoplasm (Figure 2a). Most nuclei in these cells were lightly stained, peripherally situated, and ovally shaped, indicating a relatively mature appearance. Vinculin-containing focal adhesions (FAs) were clustered in peripheral filopodia-like cell extensions in an apparent attempt to spread their cell bodies over the substrates. On the contrary, cells on the RDGC and nonpeptide surfaces displayed contracted and solid patterns without apparent nuclei contour. Being covered under undiffused cytoplasm, nuclei shape was still unable to see. Cell outlines were generally small and spheroid, with multiple rodlike projections evenly protruding outward. The ends of these pseudopodia were enlarged in the vinculin spot in a punctate circular pattern inside their margins. Cells on RDGC and nonpeptide surfaces displayed similar immature cell spreading patterns (Figure 2b and c).

Figure 3 illustrates the change of cell quantities at 1, 4, 7, 10, and 15 days. Osteoblast proliferation on RGDC surfaces increased significantly at 4 and 7 days compared with those on RDGC and nonpeptide surfaces ($P < .05$). Cell growth at 1, 10, and 15 days showed no significant difference on different surfaces. Meanwhile, osteoblast proliferation on RDGC and uncoated surfaces did not differ from each other in the whole culture process ($P > .05$).

Northern blot analysis showed an earlier OC mRNA expression on RGDC surfaces. At day 15, intense OC mRNA bands appeared and no signal occurred in the other 2 control groups (Figure 4). On day 21, OC mRNA expression stayed the same on RGDC

surfaces but began to show distinct expression in the other control groups. At this time, the mRNA levels in all groups were similar. Equal sample loading was confirmed by the unchanged density of the housekeeping gene GAPDH.

DISCUSSION

Self-assembly monolayer is a technique by which molecules under thermodynamic equilibrium conditions can spontaneously align on a surface into 2-dimensional, quasi-crystalline domains that are stable and ordered.^{10,11} When gold and silver were exposed to solution or vapors of an alkanethiol (RSH), these metals were able to bond with sulfur to form RSH self-assembly monolayer. The gold-sulfur bond was believed to be a covalent thiolate bond.⁸ In this study, titanium substrates were evaporated with a thin layer of titanium to promote the bonding with the thin film of gold. Gold surfaces are not toxic to living cells and are considered biocompatible with conditions used for cell culture.¹² This rationalized our use of gold as an experimental model surface. Of course, the most ideal approach is to immobilize the peptides on a titanium surface, but this requires much more complicated chemical approaches and instruments. The reaction is much more expensive and cannot be completed in the normal room temperature or in an efficient manner. Although, compared with titanium, gold does not possess the good biocompatibility for bone integration, this disadvantage did not affect our use of gold as in vitro model surfaces to evaluate the biological impact of peptides on osteoblasts. Peptides (RGDC, RDGC) with terminal cysteine (C) groups, which contain free thiol residues, were exposed to gold surfaces. The thiol groups, serving as anchors, covalently bonded with gold, allowing the oligopeptides to attach onto surfaces to form monolayers. Functional group RGD and RDG formed a ligand layer to cell membrane receptors. The XPS and FTIR results confirmed the

immobilization of RGD peptide onto experimental surfaces. Meanwhile, some of the symmetric peak shapes of the FTIR spectra also suggested that the molecular organization on the surfaces is highly ordered. Our procedure corresponded with some previously described similar surface modification methods using RGD grafts,¹³ and the surface identification results verified the availability of this procedure for in vitro experiments.

Endosseous integration can be broken into 3 distinct bony healing phases: osteoconduction, de novo bone formation, and bone remodeling. Osteoconduction relies on the migration and colonization of differentiating osteogenic cells on the implant surface. De novo bone formation primarily requires the recruitment of potentially osteogenic cells to the site of future matrix formation.¹⁴ When implants are surgically placed in bone bed, they are exposed to blood and extracellular fluids. Various proteins are adsorbed onto implant surfaces and then mediate different cell types to attach onto these surfaces. As anchorage-dependent cells, osteoblasts, the major osteogenic cells, can only begin their cell functions after fully attaching and spreading.^{15,16} So cell attachment and spreading are considered important indicators of biocompatibility and bioactivity of implant materials.

In the present study, cell attachment on RGDC surfaces was significantly enhanced within 8 hours after plating. At the 4-hour point, attachment rate (attachment density/seeding density) on the RGDC surface was approximately 60% rather than the 35% that appears on the RDGC and nonpeptide surfaces. At the 8-hour point, the attachment rate was 85% on RGDC surfaces rather than the 70% seen on RDGC and nonpeptide surfaces. After 12 hours, most cells in different treatment groups finished the attachment process and entered the G₁ phase, so no difference could be found among the 3 groups. Generally, these results suggested a promotional effect of RGD

peptide on osteoblast attachment, especially at the initial phase of tissue-implant contact.

Cell attachment is a complex process that includes several steps. The initial attachment is followed by the formation of FA sites and subsequent cell spreading. Focal adhesions are the largest and tightest matrix adhesions, which are highly dynamic and heterogeneous structures and represent a morphologically prominent association between integrins and the cytoskeleton.¹⁷ Vinculin is one of many prominent cytoplasmic constituents of FAs and is believed to play important roles in stabilizing cell adhesion and regulating cell shape, morphology, and mobility.¹⁸ In our experiments, the results of the cell attachment assay were paralleled with the results of cell spreading microscopy. Four hours after seeding, most osteoblasts on RGDC surfaces displayed flattened, maturely spread morphology with scattered FA, leading to intimate contact between the surface and the cell. On RDGC and nonpeptide surfaces, diffused FA could not be found and cells were not fully spread. This discrepancy in spreading dynamics provides more evidence of enhanced cell attachment on the RGDC surfaces.

The cell proliferation on the RGDC surfaces was increased at the initial stage of cell growth. After 10 days, cell proliferation on different surfaces became similar. This could be attributed to contact inhibition when most of the surfaces were occupied by cells. Enhanced proliferation of osteoblasts might advance extracellular matrix secretion, thus favoring early stabilization of implant in supporting tissue. This will undoubtedly benefit clinical outcomes of the implantation.

Osteocalcin is the marker of differentiated osteoblasts. The secretion of OC is believed to be related to the coordination of bone resorption and new bone deposition.¹⁹ It signals the beginning of the bone remodeling by promoting the maturation of the osteoclast and appears to be the only protein as-

sociated with the mineralization front.²⁰ The earlier expression of OC on RGDC surfaces provided evidence of an earlier differentiation of the osteoblasts on those surfaces. This enhanced osteoblast turnover may be significantly useful in accelerating tissue integration and inducing early anchorage.

The difference between RGDC and RDGC is the order of constitutive peptides. Although both of them had identical chemical composition and could be immobilized onto gold surfaces through Cys residues, their effects on the osteoblast functions were totally different in our experiments. This suggested a structure-dependent effect of RGD peptide rather than a composition-dependent effect. These ligand-binding properties are important for adhesion receptors such as integrins. Integrins link extracellular matrix proteins on the extracellular face of the cell membrane to cytoskeletal proteins and actin filaments on the cytoplasmic face. The short cytoplasmic domains of the α and β integrin subunits appear to function by coupling with cytoplasmic proteins that nucleate the formation of large protein complexes containing both cytoskeletal and catalytic signaling proteins, thus transmitting biochemical signals and mechanical force across the plasma membrane.⁴ The cytoskeletal linkages enable integrins to mediate cell adhesion and regulate cell shape and gene expression.²¹ Surfaces modified with RGD may trigger the integrin activation, advance or intensify subsequent signal transduction, and alter the behavior of osteoblasts. This might be the reason for the enhanced cell function on RGD surfaces in our experiments. Although no clear mechanism concerning the regulation of cell differentiation and proliferation by integrins has been identified, our results indicate the possible influence of RGD on those aspects.

Regarding the practicality of this surface modification model in *in vivo* studies, some of our pilot experiments were not in favor of this model, because, due to loose bonding between

gold film and titanium substrate, most of the coating shed as debris when specimens are prepared. The ultimate goal of this research is to firmly immobilize those bioactive peptides on titanium or titanium alloy surfaces and explore their *in vivo* effects. Fortunately, there appear to be some applicable ways to achieve this, such as the covalent coupling technique. Various methods are currently under investigation.²² Before any practical application of the proactive modification strategy can be achieved, a valid and cost-effective approach for persistent and effective delivery of bioactive agents in implant-tissue interface must be found.

CONCLUSION

We used self-assembly monolayer techniques to immobilize RGD-containing peptides on substrate surfaces. *In vitro* studies have indicated that the immobilized adhesive motif RGD not only promotes attachment and spreading of osteoblasts but also enhances the proliferation and differentiation of those cells on the test surfaces. Immobilization of RGD peptides onto implant surfaces might be an effective strategy for the development of new proactive dental implants.

ACKNOWLEDGMENT

This work was supported by the National Science Foundation of China.

REFERENCES

1. Hanns PJ. Prosthesis-bone interface. *J Biomed Mater Res (Appl Biomater)*. 1998;43:350-355.
2. Baier RE. Surface properties influencing biological adhesion. In: Manly RS, ed. *Adhesion in Biological Systems*. New York, NY: Academic; 1970:15-48.
3. Brunette DM. The effects of implant surface topography on the behavior of cells. *Int J Oral Maxillofac Implants*. 1988;3:231-246.
4. Edwin AC, Joan SB. Integrins and signal transduction pathways: the road taken. *Science*. 1995;268:233-239.
5. Puleo D, Bizios R. RGDS tetrapeptide binds to osteoblasts and inhib-

- its fibronectin-mediated adhesion. *Bone*. 1991;12:271–276.
6. Dee KC, Andersen TT, Bizios R. Osteoblast population migration characteristics on substrates modified with immobilized adhesive peptides. *Biomaterials*. 1999;20:221–227.
7. Dee KC, David C, Rueger A, Thomas T. Conditions which promote mineralization at the bone-implant interface: a model *in vitro* study. *Biomaterials*. 1996;17:209–215.
8. Mrksich M, Chen CS, Xia Y, Dike LE, Whitesides GM. Controlling cell attachment on contoured surfaces with self-assembled monolayers of alkanethiolates on gold. *Proc Natl Acad U S A*. 1996;93:10775–10778.
9. Chomczynski P, Sacchi N. Single-step method of RNA isolation by acid guanidinium thiocyanate-phenol-chloroform extraction. *Ann Biochem*. 1987;162:156–159.
10. Whitesides GM, Mathias JP, Seto CT. Molecular self-assembly and nanochemistry: a chemical strategy for the synthesis of nano-structures. *Science*. 1991;254:1312–1319.
11. Mrksich M, Whitesides GM. Using self-assembled monolayers to understand the interactions of man-made surfaces with proteins and cells. *Ann Rev Biophys Biomol Struct*. 1996;25:55–78.
12. Mrksich M, Dike LE, Tien J, Ingber DE, Whitesides GM. Using microcontact printing to pattern the attachment of mammalian cells to self-assembled monolayers of alkanethiolates on transparent films of gold and silver. *Exp Cell Res*. 1997;235:305–313.
13. Zhang S, Lin Y, Michael A. Biological surface engineering: a simple system for cell pattern formation. *Biomaterials*. 1998;115:1213–1220.
14. Davies JE. Mechanisms of endosseous integration. *Int J Prosthodont*. 1998;11:391–401.
15. Puleo DA, Holleran LH, Doremus RH, Bizios R. Osteoblast responses to orthopedic implant materials *in vitro*. *J Biomed Mater Res*. 1991;25:711–723.
16. Anselme K. Osteoblast adhesion on biomaterials. *Biomaterials*. 2000;21:667–681.
17. Burrige K, Magdalena CW. Focal adhesions, contractility, and signaling. *Annu Rev Cell Dev Biol*. 1996;12:463–519.
18. Bubeck P, Pistor S, Wehland J, Jockusch BM. Ligand recruitment by vinculin domains in transfected cells. *J Cell Sci*. 1997;110:1361–1371.
19. Heersche JNM, Reimers MS, Wrana JL, Wayne MMY, Gupta AK. Changes in expression of alpha I type I collagen and osteocalcin mRNA in osteoblasts and odontoblasts at different stages of maturity as shown by *in situ* hybridization. *Proc Finn Dent Soc*. 1992;88:173–182.
20. Nefussi JR, Brama G, Modrowski D, Oboeuf M, Forest N. Sequential expression of bone matrix proteins during rat calvaria osteoblast differentiation and bone nodule formation *in vitro*. *J Histochem Cytochem*. 1997;45:493–503.
21. Choquet D, Felsenfeld DP, Sheetz MP, et al. Extracellular matrix rigidity causes strengthening of integrin-cytoskeleton linkages. *Cell*. 1997;88:39–48.
22. Dee KC, Bizios R. Mini-review: proactive biomaterials and bone tissue engineering. *Biotechnol Bioeng*. 1996;50:438–442.